Baquerizo, L., Matschei, T., Scrivener, K.

Impact of water activity on the water content of cement hydrates

1. Introduction

Varying hydration states, i.e. water content of C-S-H, AFm and AFt phases may have a direct impact on the specific density/volume of cement paste, e.g. the volume of some hydrates can change as much as 20% during drying [1] and may thus strongly affect the porosity and performance of a cementitious system. Unfortunately a systematic study summarizing the hydration states of individual cement hydrates under related exposure conditions is still not available.

It has been demonstrated that water activity $a(H_2O)$, and thus the water chemical potential $\mu(H_2O)$ plays an important role in the prediction of the final phase assemblage of cementitious systems. For example Albert et al. [2] and Monteiro [3] have shown, e.g., that decreasing the water chemical potential by reducing water vapor pressure (RH) or increasing temperature destabilize ettringite and monosulfoaluminate becomes more stable. The aim of this paper is to demonstrate that a decrease in the water chemical potential of a cementitious system can lead to changes of the hydration states of crystalline cement hydrates (AFm and AFt phases). Furthermore the paper summarizes experimentally determined hydration states of the aforementioned hydrates at 25°C and different RH's in order to enable later calibration of a thermodynamic model to predict the impact of water activity on phase assemblages and the distribution of water amongst them.

AFm (Al_2O_3–Fe_2O_3–mono) phases are hydrated tetracalcium aluminate compounds belonging to the lamellar double hydroxide family. They occur during the hydration process of Portland cements and are composed of positively charged main layers $[Ca_2Al(OH)_6]^+$ and negatively charged interlayers $[X.nH_2O]^-$ where X is either one monovalent anion or half a divalent anion. A crystal may contain more than one species of X anions. The layer thickness c' depends on the nature of the X anion and the amount of interlayer water n [4]-[5]. The most important AFm phases are presented in Table 1; the interlayer anion is shown in bold italic font and the interlayer water content is denoted by "n". Previous studies about hydration states of the aforementioned AFm phases can be found in the references listed in Table 1.

AFt (Al_2O_3-Fe_2O_3-tri) phases have the general formula $[Ca_3(Al,Fe)(OH)_6 \cdot 12H_2O]_2 \cdot X_3 \cdot nH_2O$, where n is the interchannel water and X represents usually one formula unit of a doubly charged anion. The most important AFt phase is ettringite $[Ca_3(Al)(OH)_6]_2(SO_4)_3 \cdot 26H_2O$ or $C_6A\hat{S}_3H_{32}$. From the theoretical 32 water molecules, 2 are located in the interchannel space and can be removed at room temperature and low RH, even though some discrepancies exist about the real amount of interchannel water and whether it can be removed or not at these conditions [6]-[9].

Table 1:
Most important AFm phases and reported water content at room temperature

Phase Name	Chemical formula	Cement notation	Ref.
Monosulfo-aluminate	$[Ca_4(Al)_2\,(OH)_{12}]^{2+}\,[\boldsymbol{SO_4}\cdot nH_2O]^{2-}$ n=4,6,8,10	$C_4A\hat{S}H_{6+n}$	[6][10]-[16]
Hydroxy-AFm	$[Ca_4(Al)_2\,(OH)_{12}]^{2+}\,[\boldsymbol{(OH)_2}\cdot nH_2O]^{2-}$ n=4,6,12	C_4AH_{7+n}	[17]-[19]
Monocarbo-aluminate	$[Ca_4(Al)_2\,(OH)_{12}]^{2+}\,[\boldsymbol{CO_3}\cdot nH_2O]^{2-}$ n=5	$C_4A\hat{C}H_{6+n}$	[16]-[17], [20]-[22]
Hemicarbo-aluminate	$[Ca_4(Al)_2\,(OH)_{12}]^{2+}\,[\boldsymbol{1/2CO_3(OH)}\cdot nH_2O]^{2-}$ n=5.5	$C_4A\hat{C}_{0.5}H_{6.5+n}$	[16]-[17], [23]

2. Experimental procedure

3.1. Materials

All chemicals used were analytical grade reagents. The precursor used in the synthesis of AFm and AFt phases was tricalcium aluminate C_3A, which was prepared from a 3:1 molar ratio of $CaCO_3$ and Al_2O_3 at 1400°C, based on the procedure given by Matschei [24]. Anhydrite $CaSO_4$ was prepared by dehydration of gypsum in a muffle furnace at 550°C overnight. CaO was obtained by decarbonation of $CaCO_3$ at 1000°C overnight. Double distilled CO_2 free water was used in the synthesis of the hydrates. NaOH with purity higher than 99% was used in the experiments with solutions at high ionic strength.

3.2. Synthesis and aging of AFm and AFt phases

The synthesis procedures were based on the protocols followed by Matschei [24]. A closed sample holder was used to avoid carbonation during purity checking of wet hydrate slurries by XRD. A displacement correction of the peaks in the pattern was done by using Rutile TiO_2 as internal standard. The reactants and the synthesized phases are shown in Table 2. The synthesis time was 4 weeks. Once purity has been confirmed, the solid was vacuum filtered under N_2 atmosphere and aged at 25°C inside hermetic glass bottles equilibrated with salt solutions at different RH: Na(OH)= 8%, CH_3CO_2K= 23%, $MgCl_2$=33%, $Mg(NO_3)_2$=51.5%, NaCl= 74%, KCl= 83%, K_2SO_4= 97%, H_2O= 100%. The aging periods were 10 months in the case of Monosulfoaluminate and 8 months for the other phases.

To study the impact of temperature in the re/de-hydration behavior of cement hydrates, Monosulfoaluminate synthesis was performed at 5°C, 25°C, 50°C and 85°C.

In order to study the impact of the ionic strength of the solution in the dehydration behavior of Hydroxy-AFm, OH19-AFm (the index 19 shows the total water content of the phase) initially synthesized at 5°C was mixed with NaOH solutions at 3 different concentrations (2, 3 and 4 mol) at 25°C. The XRD measurements were done in wet filtered samples after 3 days of exposure to the alkali solution.

Table 2:
Used recipes to synthesize AFm and AFt phases

	Cement notation	*Name and Abbreviation*	*Reactants*	*w/s*	*Temp (°C)*
AFm	$C_4A\hat{C}H_{11}$	Monocarboaluminate (Mc)	$C_3A+ CaCO_3$ / 1 : 1	10	23
	$C_4A\hat{C}_{0.5}H_{12}$	Hemicarboaluminate (Hc)	$C_3A+ CaCO_3+CaO$ / 1 : 0.5 : 0.5	10	23
	$C_4A\hat{S}H_{14}$	Monosulfoaluminate (Ms)	$C_3A+ CaSO_4$ / 1 : 1	20	85
	C_4AH_{19}	Hydroxy-AFm (OH-AFm)	$C_3A+ CaO$ / 1 : 1	10	5
AFt	$C_6A\hat{S}_3H_{32}$	Ettringite (Ett)	$C_3A+ CaSO_4$ / 1 : 3	20	23

3.3. Characterization

X-ray analyses of wet and dried samples were carried out with a Bruker D8 Advance diffractometer (CuKα radiation, 45 mA, 35 kV) equipped with a Super Speed detector, in the range 7-50° 2θ, with a step size and time per step of 0.02° and 0.5 s, respectively. A closed sample holder was used to avoid carbonation and drying during testing.

Thermogravimetry measurements were performed using a Mettler Toledo TGA/SDTA 851^e under N_2 flux, over the range 25°-1100°C, with a heating rate of 20°C/min. The measurements were done immediately after sample preparation to avoid drying and carbonation.

3. Results and discussion

3.1. Water chemical potential as function of RH, temperature and solution ionic strength

The aim of the present paper is to demonstrate that **changes of the water chemical potential $\mu(H_2O)$ will impact the interlayer/interchannel water content of sensitive cement hydrates e.g. AFm and AFt**, . This may lead to de- or rehydration processes which consequently impact the specific solid volume of the hydrates and potentially the performance of the used binder system.

Here the chemical potential measures the driving force for movement of water molecules between two sites. The chemical potential of water is related to the change in the Gibbs free energy of the system, which depends on the pressure, temperature and species in solution. The water chemical potential under atmospheric conditions as function of temperature can be defined as follows:

$$\mu(H_2O)_{l,T} = \mu°(H_2O)_l + RTln(a(H_2O)) \quad Eq.\ 1$$

where $\mu°(H_2O)_l$ is the standard chemical potential of liquid water at 298.15 K, R is the gas constant 8.314 J/(K mol), T is the temperature in K and $a(H_2O)$ is activity of water which can be linked to relative humidity RH at a given water vapor pressure p and known saturation vapor pressure of water p^o according to Raoult's law by:

$$a(H_2O) = \frac{p}{p^\circ} = \frac{RH}{100} \qquad Eq.\ 2$$

In simple words according to the equations shown above there are 2 ways to change $\mu(H_2O)$: by **changing the $a(H_2O)$, i. e. $\frac{RH}{100}$ at constant temperature** (Fig. 1a) **and by adjusting the temperature at constant $a(H_2O)$** (Fig. 1b).

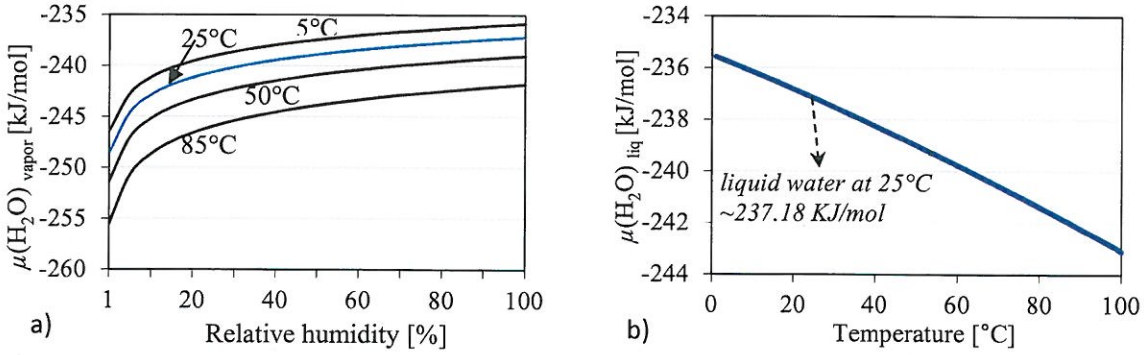

Fig. 1. Water chemical potential at: a) different isotherms as function of RH and b) in saturated conditions as function of temperature.

Another way to **decrease the $a(H_2O)$** and thus the $\mu(H_2O)$ **can be achieved by increasing the ionic strength of the solution** by dissolving ionic compounds (in our case NaOH was used). The Pitzer model was used to quantify the changes of water activity as function of ionic strength. This model is one of the most used methods for calculating ion activity coefficients in concentrated electrolyte solutions at room or elevated temperatures. Even though the method is semi-empirical it is based on rigorous thermodynamic definitions of the chemical potential of the species, the osmotic pressure and the potential energy between ions [25]. For a solution of a single electrolyte MX the activity coefficient may be expressed as [26]:

$$ln\,\gamma = |Z_M Z_X| f^\gamma + m\frac{2\nu_M\nu_X}{\nu} B^\gamma_{MX} + m^2\left(\frac{2(\nu_M\nu_X)^{3/2}}{\nu}\right) C^\gamma_{MX} \qquad Eq.\ 3$$

where ν_M and ν_X are the numbers of M and X ions in the formula unit and Z_M and Z_X their charges. m is the molality of the solution and $\nu = \nu_M + \nu_X$. As it is not the aim of this work to explain the detailed Pitzer model the reader is referred to [25]. Fig. 2 shows the calculated relation between NaOH molality and its impact on water activity. It can be seen that concentrated NaOH solutions have the potential to significantly decrease the $a(H_2O)$. Its impact on the hydration states of cement hydrates will be shown later.

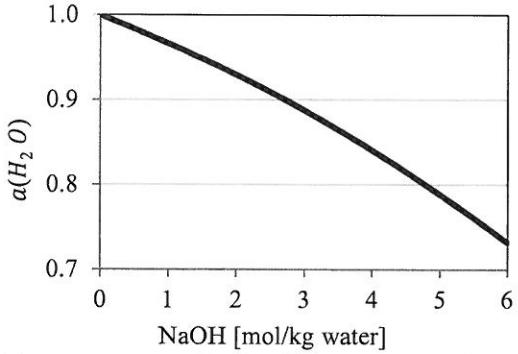

Fig. 2. Calculated water activity [$a(H_2O)$] at 25°C as function of NaOH molality

Using the three mentioned procedures as a reference to decrease the $\mu(H_2O)$ a series of experiments were done in order to demonstrate its influence in the hydration states of AFm and AFt phases.

3.2. Impact of water chemical potential on the hydration states of AFm phases.

3.2.1. Impact of RH and temperature on Monosulfoaluminate

As shown in the X-ray difractograms Fig.3a at 25°C, Ms14 (the index 14 shows the total water content of the phase) is the observed hydration state at saturated conditions but it starts to dehydrate at 97% RH to Ms12 which is found until 23%RH (Ms12 water content was confirmed by TGA). At 8%RH a lower hydration state appears with a basal space of 8.15Å, which according to Dosch et al. [12] corresponds to Ms10, but according to our TGA results the hydration state is Ms10.5. As can be seen in Fig. 3b a decrease of RH may lead to significant reduction of specific solid volume of monosulfoaluminate of up to 15%, which may in turn affect the space filling properties of hydrated cements significantly.

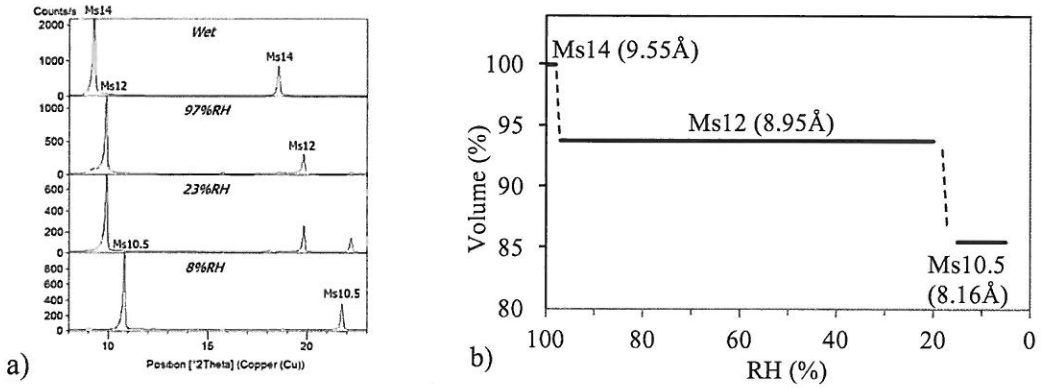

Fig. 3. a) XRD patterns of Ms14 dried at 25°C and different RH's. b) Volume changes and different hydration states of Ms as function of RH at 25°C (basal space in parenthesis).

In a second experiment the impact of temperature on the hydration states of monosulfoaluminate at saturated conditions was investigated. It was found that in the range from 25 to 85°C Ms14 was observed. However at low temperatures (5°C) a water rich hydrate state was identified by XRD which we attributed to Ms16 (Fig. 4). Also when initially synthesized Ms14 is stored at 5°C it rehydrates to Ms16, but will subsequently dehydrate to Ms14 if exposed at temperatures higher than 25°C (exact temperature was not determined). Hence we can conclude that lower temperatures tend to stabilize higher hydration states of Monosulfoaluminate due to an increase in the $\mu(H_2O)$ (See Fig. 1b).

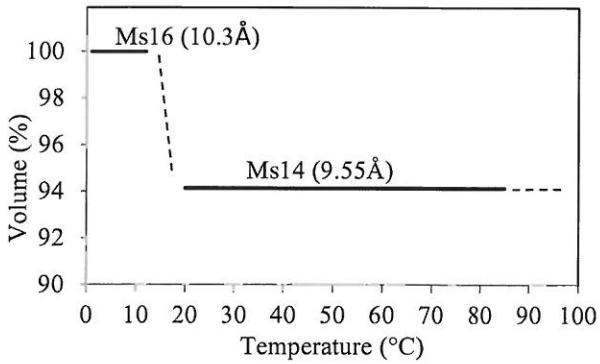

Fig. 4. Volume changes and different hydration states of Ms at saturated conditions as function of temperature (basal space in parenthesis).

3.2.2. Impact of RH and solution ionic strength on Hydroxy-AFm

At 25°C, OH19-AFm is found until 97%RH and then completely dehydrates to OH13-AFm at 83%RH. OH13-AFm is observed until 23%RH. At 8%RH Hydroxy-AFm further dehydrates and OH11-AFm is formed. An exact quantification of the water content could not be done in any of the aged samples since a high degree of carbonation as well as decomposition due to thermodynamic constraints was obtained, resulting in the precipitation of other phases such as Hemicarboaluminate, Hydrogarnet (Hg) and Portlandite (CH), which hampers the analysis.

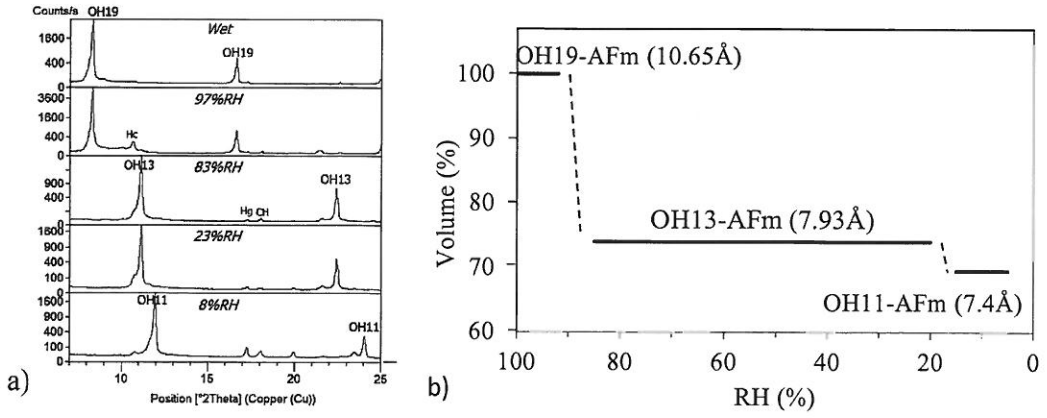

Fig. 5. a) XRD patterns of OH19-AFm dried at 25°C and different RH's. b) Volume changes and different hydration states of OH-AFm as function of RH at 25°C (basal space in parenthesis)

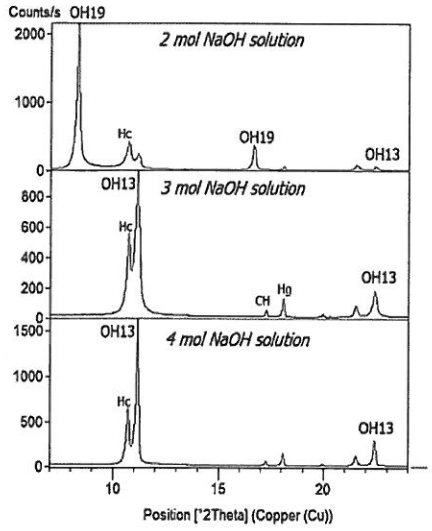

Fig. 6. XRD patterns of wet OH-AFm at different NaOH mol concentrations at 25°C.

As stated in chapter 3.1 a third way to manipulate the chemical activity of water is to increase the ionic strength of the electrolyte solution. This was done by dissolving NaOH in water at different molalities. When initially synthesized OH19-AFm is mixed with the NaOH solutions, it dehydrates to OH13-AFm at a concentration of 3 mol NaOH (Fig. 6). According to the calculated water activity using the Pitzer model [25] (Fig. 2), the water activity at 3 mol NaOH is 0.89, which is sufficient to destabilize the highest hydration state of OH-AFm. Note that this water activity corresponds to 89% RH. Thus a comparison with the observed dehydration behavior of OH-AFm at decreasing RH's (See Fig. 5) agrees well with the obtained data at increasing ionic strengths. Additionally Hemicarboaluminate is observed in all the patterns, since the used NaOH contained carbonate impurities (less than 1% Na_2CO_3).

3.2.3. Impact of RH on carboaluminate phases (Monocarboaluminate and Hemicarboaluminate) at 25°C

As demonstrated in Figs 7a and 7b Monocarboaluminate shows no change in its hydration states from 100% to 8%RH. The 11 H_2O state ,Mc11, was observed . The measured basal space is 7.57Å.

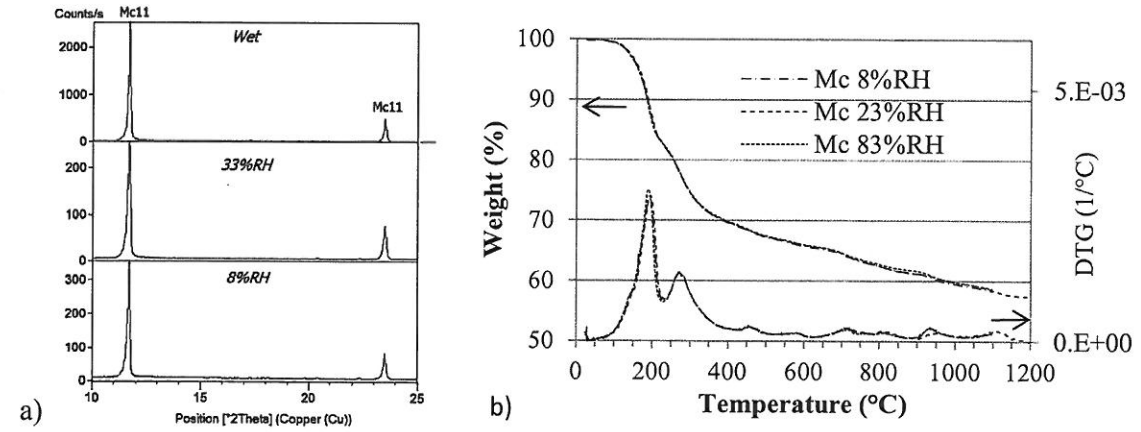

Fig. 7. a) XRD patterns of Mc equilibrated at 25°C and different RH's. b) TGA of Mc pre-conditioned at 8%, 23% and 83% RH at 25°C .

Hemicarboaluminate Hc12 (8.205Å) is detected from 100% to 33%RH. The water content was confirmed by TGA. A peak with a lower basal space (7.81Å) starts to appear at 23%RH, which increases in intensity at 8%RH. This suggests an additional hydration state of hemicarbolauminate appearing at RH's <33%. The water content of this lower hydration state of Hc could not been determined since the initial Hc12 has not been completely dehydrated.

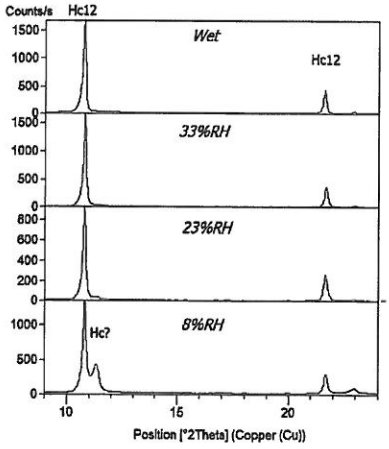

Fig. 8. a) XRD patterns of Hc pre-conditioned at 25°C and different RH's

As shown before carboaluminate AFm phases (especially Mc) appear to be stable along a wide range of $\mu(H_2O)$ and are thus relatively robust against changing exposure conditions i.e. at differing humidities and temperatures; the latter is still under investigation. Compared to other AFm phases e.g. OH-AFm and Ms, the structure of Mc differs significantly which may impact the stability of this phase significantly. In Mc one Oxygen atom of the carbonate (CO_3^{2-}) group is directly linked to a Ca atom of the main layer and in addition the remaining Oxygen atoms of this carbonate group contribute to the formation of hydrogen bonds with water molecules, providing a strong cohesion between inter- and main layer. This may be a plausible explanation why monocarboaluminate is comparatively stable over a wide range of exposure conditions [20].

3.3. Impact of RH on AFt phases (Ettringite) at 25°C.

Etringite is the cement hydrate with the highest specific solid volume and water content. AFt has a channel column structure. Theroretically only 2 of its water molecules are relatively loosely bound in the interchannel spaces and may therefore be relatively easily removed during drying. Nevertheless our investigations showed that ettringite is relatively unsensitive against changing water activities or RH's at 25°C. The X-ray patterns of samples aged for 8 months at a given humidity showed no obvious changes within the range 100% - 8%RH (no shift or displacement of the main reflections). Additional TGA experiments to determine the water content of Ettringite showed that it varied from 31.9

H_2O molecules at 97%RH to 31.02 H_2O molecules at 8%RH (See Fig. 9) which suggests the removal of maximim one molecule from the interchannel. In summary it was shown that despite its high water content ettringite remains very robust againts changing relative humidities at 25°C. The impact of temperature remains subject of further investigations.

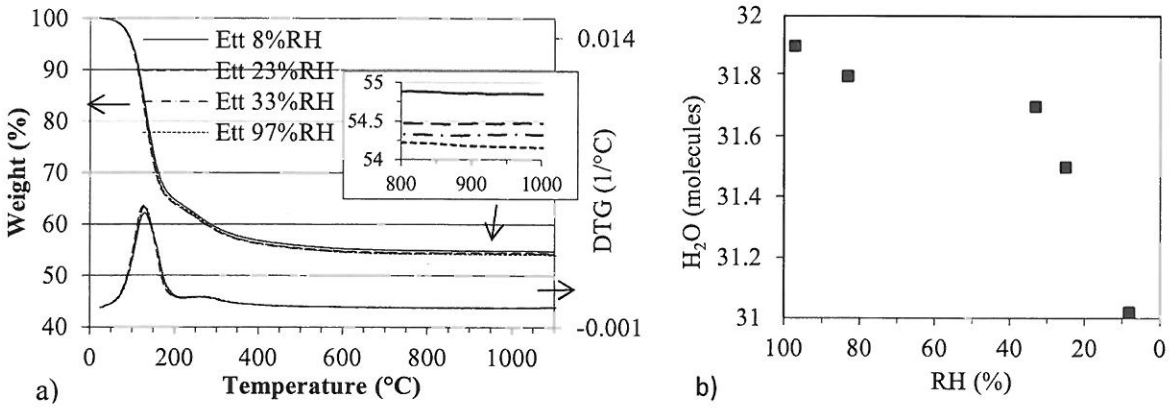

Fig. 9. a) TGA of Ett dried at 25°C and different RH's. b) Experimental water content of Ett at 25°C.

4. Conclusions

Aim of this study was to show the impact of changing water chemical potential as function of i) humidity, ii) temperature and iii) ionic strength of an electrolyte on the mineralogy of hydrated cements. The three methods used to change the water chemical potential resulted in significant differences of the hydration states and thus the bound water content of cement hydrates. It was shown that we can group the AFm and AFt phases according to their sensitivity against changing water chemical potentials: **Sensitive** phases are Monosulfoaluminate and Hydroxy-AFm, **less sensitive** hydrates are Hemicarboaluminate and Ettringite, and Monocarboaluminate is an apparently **non-sensitive** phase. The identified sensitive phases show specific solid volume changes of up to 30%, whereas the volume of non-sensitive phases remains unchanged in the investigated range between 8 and 100% humidity.

The results let us conclude that minor structural differences e.g. the direct bond of the interlayer carbonate group to the calcium of the main layer of monocarboaluminate, may have a strong impact on the stability of the phases with respect to changing water vapor pressures RH's under isothermal conditions.

Thus as a consequence of this work certain phases assemblages can be identified, which appear to be more robust against changing environmental exposure conditions involving

wetting and drying. For example phase assemblages containing monocarboaluminate and ettringite are dimensionally very stable across a wide range of humidities, which indicates that hydrated limestone blended cements may be less affected by water activity induced specific solid volume changes. At the moment it remains questionable whether we can easily link the results to concrete performance properties e.g. shrinkage, strength etc. Nevertheless it enables us to engineer phase assemblages which are from a mineralogy point of view less sensitive to changes of exposure conditions.

Our results also showed that systems with high ionic strengths e.g. alkali activated binders which present a high ionic strength pore solution may precipitate hydrates with lower water content than at high water activities. Also as the water activity in these systems may change significantly over time, initially formed phases with high water content may dehydrate subsequently due to an increase in ionic strength of the pore solution caused by the consumption of water during hydration.

Further research will be done to incorporate the findings into a thermodynamic model, capable of predicting the volume stability of a cementitious system during exposure at different external conditions. Unfortunately our insufficient knowledge of the impact of $\mu(H_2O)$ on the water content of C-S-H hinders the analysis of a more realistic cementitious system containing Portland cement, currently. However missing relevant data regarding water content of C-S-H will be obtained in the course of ongoing work in the frame of the Nanocem - Transcend projects [27].

5. Acknowledgement

The research leading to these results has received funding from the European Union Seventh Framework Programme (FP7 / 2007-2013) under grant agreement 264448.

We would like to thank Holcim Group Support Ltd. for actively promoting cement research, especially the Innovation Function and the Analytical Lab of the Materials Technology Department.

6. References

[1]. Baquerizo, L., Matschei, T., Scrivener, K., The impact of water chemical potential on the hydration states of Monosulfoaluminate, 31th Cement and Concrete Science Conference, London, 2011.

[2]. Albert, B., Guy, B., Damidot, D., Water chemical potential: A key parameter to determine the thermodynamic stability of some hydrated cement phases in concrete?, Cem. Concr. Res. 36, 2006, 783-790.

[3]. Monteiro, J.F.P., Chemical potential diagrams as guideline for phase stability and reactivity in cementitious systems, Master Thesis, Universidade de Aveiro, 2009.

[4]. Taylor, H.F.W., Cement Chemistry, 2nd edition. Thomas Telford, London 1997.
[5]. Taylor, H.F.W., Crystal structures of some double hydroxide minerals, Mineralogical Magazine 39, 377, 377-389, 1973.
[6]. Pöllmann, H., Characterization of Different Water Contents of Ettringite and Kuzelite, proc. XII International Congress on the Chemistry of Cement, 8–13 July 2007, Montreal, Canada, 2009.
[7]. Zhou, Q., Lachowski, E.E., Glasser, F.P., Metaettringite, a decomposition product of ettringite, Cem. Concr. Res. 34, 2004, 703-710.
[8]. Zhou, Q., Glasser, F.P., Thermal stability and decomposition mechanisms of ettringite at <120°C, Cement and Concrete Research 31, 2001, 1333-1339.
[9]. Renaudin, G., Filinchuk, Y., Neubauer, J., Goetz-Neunhoeffer, F., A comparative structural study of wet and dried ettringite, Cem. Concr. Res. §40, 2010, 370-375.
[10]. Allmann, R., Refinement of the hybrid layer structure $[Ca_2Al(OH)_6]^+ \cdot [1/2SO_4 \cdot 3H_2O]^-$. Neues Jahrbuch für Mineralogie Monatshefte, 1977, 136-144.
[11]. Allmann, R., Die Doppelschichtstruktur der plättchenförmigen Calcium-Aluminium-Hydroxysalze am Beispiel des $3CaO \cdot Al_2O_3 \cdot CaSO_4 \cdot 12H_2O$. Neues Jahrbuch für Mineralogie Monatshefte, 1968, 140-144.
[12]. Dosch W., Keller H., Strassen H., 5th ISCC, Vol 2, pag 72, 1969.
[13]. Damidot, D., Glasser, F.P., Thermodynamic investigation of the $CaO-Al_2O_3-CaSO_4-H_20$ at 50°C and 85°C, Cem. Concr. Res. 22, 1992, 1179-1191
[14]. Clark, B.A., Brown, P.W., The formation of calcium sulfoaluminate hydrate compunds Part II, Cem. Concr. Res. 30, 2000, 233-240.
[15]. Kuzel, H.J., Initial Hydration Reactions and Mechanisms of Delayed Ettringite Formation in Portland Cements, Cement and Concrete Composites 18, 1996, 195-203
[16]. Pöllmann, H., Die Kristallchemie der Neubildungen bei Einwirkung von Schadstoffen auf hydraulische Bindemittel. PhD-Thesis, University of Erlangen-Nuernberg, 1984.
[17]. Fischer, R., Kuzel, H.J., Reinvestigation of the system $C_4A.nH_2O$ - $C_4A \cdot CO_2 \cdot nH_2O$, Cem. Concr. Res. 12, 1982, 517-526.
[18]. Buttler, F.G., Glasser, D., Taylor, H.F.W., Studies on $4CaO \cdot Al_2O_3 \cdot 13H_2O$ and the Related Natural Mineral Hydrocalumite, Journal of the American Ceramic Society 42, 1959, 121-126.
[19]. Robert M.H., Calcium Aluminate Hydrates and Related Basic Salt Solid Solutions, 5th ISCC, Vol 2, pag 104, 1970.
[20]. Francois, M., Renaudin, G., Evrard, O., A Cementitious Compound with Composition $3CaO \cdot Al_2O_3 \cdot CaCO_3 \cdot 11H_2O$, Acta Cryst. C54, 1998, 1214-1217.
[21]. Renaudin, G., Francois, M., Evrard, O., Order and disorder in the lamellar hydrated tetracalcium monocarboaluminate compound, Cem. Concr. Res. 29, 1999, 63-69.
[22]. Moon, J., Oh, J.E., Balonis, M., Glasser, F., Clark, S.M., Monteiro, P., High pressure study of low compressibility tetracalcium aluminum carbonate hydrates $3CaO \cdot Al_2O_3 \cdot CaCO_3 \cdot 11H_2O$, Cem. Concr. Res. 2012, 105-110.
[23]. Moon, J., Oh, J.E., Balonis, M., Glasser, F., Clark, S.M., Monteiro, P., Pressure induced reactions amongst calcium aluminate hydrate phases, Cem. Concr. Res. 41, 2011, 571-578.

[24]. Matschei, T., Thermodynamics of Cement Hydration, PhD Thesis, University of Aberdeen, 2007.
[25]. Pitzer, K.S. (editor) (1991). *Activity coefficients in electrolyte solutions* (2nd ed.). C.R,C. Press. ISBN 0-8493-5415-3. Chapter 3. *Pitzer, K.S. *Ion interaction approach: theory and data correlation*, pp. 75–153.
[26]. Grenthe, I., Wanner, H., Guidelines for the Extrapolation to Zero Ionic Strength, Report NEA-TDB-2.1, OECD Nuclear Energy Agency, Data Bank, F.91191 Gif-sur-Yvette, France, 1989
[27]. http://www.nanocem.org/index.php?id=282

Authors

Dipl.-Ing. Luis Baquerizo
Innovation, R&D
Holcim Group Support
5133 Holderbank,
Switzerland

Dr. Thomas Matschei
Innovation, R&D
Holcim Group Support
5133 Holderbank,
Switzerland

Prof. Karen Scrivener
EPFL-LMC
Holcim Group Support
1015 Lausanne,
Switzerland